Results in Nonlinear Analysis 9 (2026) No. 1, 204–220
https://doi.org/10.31838/rna/2025.08.04.014
Available online at www.nonlinear-analysis.com

Results in Nonlinear Analysis
ISSN 2636-7556

Peer Reviewed Scientific Journal

# Spectral graph topology with technical indicators for stock market regime detection

M. Sangeetha[1], M. Babu[2]

[1]Research Scholar, Department of Mathematics, VELS Institute of Science, Technology and Advanced Studies (VISTAS), Chennai, Tamil Nadu, India. [2]Assistant Professor, Department of Mathematics, VELS Institute of Science, Technology and Advanced Studies (VISTAS), Chennai, Tamil Nadu, India.

**Abstract**

The financial markets generate an abundance of technical signals, such as price, momentum, volatility, volume and S/R levels, that are used to capture the activity of traders across time. Although spectral graph clustering of sliding-window feature vectors has been shown to be better at detecting market regime than traditional baselines, existing methods limit feature space to mean return and realised volatility and neglect much of the information contained in popular technical indicators. This paper considers the Indicator-Weighted Similarity Graph (IWSG) a principled extension of the Temporal Similarity Graph (TSG) where each 8-day window is represented by a 14-dimensional feature vector containing: Bollinger Band Width, %B, Relative Strength Index (RSI), MACD histogram, Stochastic %K/%D, Commodity Channel Index (CCI), Average True Range (ATR), On-Balance Volume (OBV), and fractal support/resistance proximity score. A feature-adaptive Gaussian kernel on this space produces the IWSG adjacency matrix whose symmetric normalised Laplacian is proved positive semi-definite by means of an extended Dirichlet form argument, which provides richer spectral embedding. In experiments using ten NIFTY 50 constituents (January 2019–December 2023), the IWSG performs better than the baseline TSG model in clustering by silhouette, Davies–Bouldin, time consistency, and Calinski–Harabasz.

*Mathematics Subject Classification (2020):* 05C50, 91G70, 62H30

*Key words and Phrases:* Technical indicators; Bollinger Bands; RSI; MACD; support and resistance; spectral graph theory; graph Laplacian; market regime detection; Gaussian kernel; NIFTY 50; sliding-window clustering.

*Email addresses:* msdsangi1725@gmail.com (M. Sangeetha); mbabu5689@gmail.com (M. Babu)

*Received May 19, 2026; Accepted June 3, 2026; Online July 21, 2026*

## 1. Introduction

Market regime detection is one of the core areas of quantitative finance. Knowing whether the market is bullish, bearish, sideways, high volatility, or a "pre-breakout squeeze" determines the type of trading strategy to adopt, risk-parameter adjustments to be made, and portfolio adjustments to be made [6, 5].

### *1.1. Context from Preceding Chapters*

In chapter 1, constructed the Temporal Similarity Graph (TSG) from 8-day sliding windows of NIFTY 50 closing prices. In each window, I represented a two-dimensional feature vector of mean return and realised volatility. I plugged the Gaussian kernel on these features and computed TSG adjacency. The decomposition of the symmetric normalised Laplacian and eigen-gap resulted in dominant market regimes (bullish, bearish, mixed/volatile) with silhouette score and consistency across ten NIFTY 50 stocks.

Chapter 2 extended this framework to a four-layer domestic multiplex – price correlation, volume co-movement, news-sentiment alignment, and GICS sector affiliation – over the NSE 500. The MSGNN-EWI architecture fused these layers through adaptive cross-layer attention and achieved macro- in binary crisis detection with spectral early warning signals appearing 10–15 trading days before labelled crises.

### *1.2. Motivation: The Indicator Information Gap*

Both of the preceding chapters address feature extraction based solely on statistical summaries of price returns (mean, variance) or related asset classes. Professionals, but, often use a much richer set of data: technical analysis (TA) provides a formal vocabulary for encoding market microstructure signals that stock-price moments cannot capture:

- Bollinger Band Width (BBW) measures current volatility relative to a trailing base, indicating "squeeze" conditions before a breakout.
- RSI quantifies the balance of buying and selling pressure since the last update. It identifies extremes of overbought/oversold that often coincide with regime shifts.
- A MACD histogram captures the change in momentum over two time periods at the same time, and could indicate a signal of trend exhaustion or acceleration.
- Support/Resistance (S/R) proximity identifies price zones with historical buying or selling pressure that has consistently turned prices, two windows "near the same support level" is more behaviourally similar than two windows with only similar mean returns.
- ATR, OBV, CCI, Stochastic encode intraday volatility range, volume momentum, cyclical oscillation, and price position in the volatility range in recent time aspects of market dynamics invisible to closing-price-only features. These signals are integrated into a spectral graph framework, yielding two practical improvements: (i) a more complete market regime characterization featuring five different market phases including a breakout phase not captured in the TSG; (ii) an indicator based edge topology that better preserves the behavioural coherence between time windows.

### *1.3. Principal Contributions*

1. A 14-dimensional indicator feature map, where all the mutual complementary TA indicator indices are precisely defined, and a Z-score normalisation scheme (Section 3).
2. Indicator-Weighted Similarity Graph (IWSG), a feature-adaptive Gaussian kernel and a fractal-based Support/Resistance edge-weight augmentation (Section 4).

3. Extension of the spectral validity theorem of Chapter 1, to high-dimensional indicator feature spaces, by proving 3.8, a positive semi-definiteness theorem for the IWSG Laplacian.
4. A Support/Resistance Graph Topology Theorem, which states that the S/R proximity weights are the ones that bring more intra-cluster edges at historically significant price levels (Theorem 6.1). A five-regime spectral structure result is presented that a breakout regime is present in the IWSG in addition in addition to the standard bullish/bearish/sideways/volatile regimes (Section 5. Experimental results for ten NIFTY 50 stocks when evaluated on all four regime-quality metrics (Section 9) against five baselines, which is superior to IWSG.

## 2. Literature Review

### *2.1. Technical Analysis and Market Regimes*

Technical analysis has a long history in financial research. Brock et al. [6] showed that simple moving-average and trading-range break rules generate returns not explained by standard equilibrium models. Lo et al. [5,17] demonstrated that chart patterns carry statistically significant predictive content beyond linear time-series models. Naz´ario et al. [7] reviewed 85 empirical studies on moving-average rules and found significant out-of-sample profitability in 59% of cases across equity, commodity, and currency markets. In the deep-learning context, Sezer et al. [8, 18] surveyed architectures incorporating TA indicators and found consistent accuracy improvements when RSI, MACD, and Bollinger Bands are included.

### *2.2. Graph-Theoretic Methods in Finance*

The use of MSTs for hierarchical structure extraction from stock correlation matrices was the first work by Mantegna [4]. Esmalifalak and Moradi-Motlagh [9] surveyed correlation network approaches in economics and finance. Wei et al. [10,14] proposed FSTGAT, a spatiotemporal graph attention network capturing dynamic inter-stock relationships. The TSG of Chapter 1 [1] and the MSGNN-EWI of Chapter 2 [2] are the direct predecessors of the IWSG.

### *2.3 Support and Resistance in Quantitative Research*

Support and resistance levels represent price zones where historical buying or selling pressure has repeatedly reversed trends. Osler [11,15] provided empirical evidence that S/R levels at round numbers predict intraday exchange-rate reversals. Leon and Odasso [12,16] proposed algorithmic S/R detection using local extrema in price series. The incorporation of S/R proximity into a graph edge weight formalising the intuition that windows near the same support are behaviourally more similar is novel to the present work.

### *2.4 Gap Addressed*

None of the cited works integrates the full suite of TA indicators (Bollinger Bands, RSI, MACD, Stochastic, CCI, ATR, OBV) with support/resistance detection within a spectral graph-theoretic clustering framework. This chapter addresses that gap directly and provides the theoretical bridge from domestic indicator topology to the international Balanceof- Payments layer of Chapter 4.

## 3 Technical Indicator Feature Map

Let $P=\{p_1, \ldots, p_T\}$ be a closing-price series with associated high prices $\{H_t\}$, low prices $\{L_t\}$, and volume $\{V_t\}$. For each 8-day sliding window $W_i=\{p_i, \ldots, p_{i+7}\}$ we compute the following indicators evaluated at the last day $t=i+7$, then Z-score normalise each feature dimension across all n windows.

*3.1 Mean Return and Realised Volatility (Inherited)*

**Definition 3.1 (Mean Return and Volatility).** The log-return is $r_t = log\left(p_t / p_t - 1\right)$.

$$\alpha_i = \frac{1}{8}\sum_{t=i}^{i+7} r_t; \; \beta_i = \sqrt{\frac{1}{8}\sum_{t=i}^{i+7}\left(r_t - \alpha_i\right)^2}$$

*3.2 Bollinger Band Width and %B Position*

**Definition 3.2 (Bollinger Bands).** With rolling window $q = 20$ and multiplier $m = 2$:

$$SMA_{20}(t) = \frac{1}{20}\sum_{s=t-19}^{t} p_s; \qquad \sigma_{20}(t) = \sqrt{\frac{1}{20}\sum_{s=t-19}^{t}\left(p_s - SMA_{20}(t)\right)^2}$$

$$BBW_i = \frac{2m\sigma_{20}(i+7)}{SMA_{20}(i+7)}; \qquad (\%B)_i = \frac{p_{i+7} - \left(SMA_{20} - m\sigma_{20}\right)}{2m\sigma_{20}(i+7)} \tag{1}$$

A small $BBW_i$ (“Bollinger squeeze”) signals pre-breakout conditions. A $(\%B)_i$ near 0 or 1 indicates price at the lower or upper band.

*3.3 Relative Strength Index (RSI)*

**Definition 3.3 (RSI).** Let $U_t = max\left(p_t - p_{t-1}, 0\right)$, $D_t = max\left(p_{t-1} - p_t, 0\right)$. With $q = 14$:

$$RSI_i = 100 - \frac{100}{1 + \frac{EMA_{14}(U)_{i+7}}{EMA_{14}(D)_{i+7}}} \tag{2}$$

*scaled to* [0, 100]. *Values above 70 signal overbought; below 30 signal oversold conditions.*

*3.4 MACD, Signal Line, and Histogram*

**Definition 3.4 (MACD).** *With fast period* $q_1 = 12$*, slow period* $q_2 = 26$*, signal period* $q_3 = 9$*:*

$$\begin{gathered} MACD_i = EMA_{12}(p)_{i+7} - EMA_{26}(p)_{i+7}, Sig_i = EMA_9(MACD)_{i+7}, \\ Hist_i = MACD_i - Sig_i. \end{gathered} \tag{3}$$

A positive and growing $Hist_i$ confirms bullish momentum; a negative and deepening $Hist_i$ confirms bearish momentum.

*3.5 Stochastic Oscillator*

**Definition 3.5 (Stochastic %K and %D).** Over look-back **q = 14**:

$$(\%K)_i = 100.\frac{p_{i+7} - SMA_{12}(PT)_{i+7}}{max_{s\in[i-6,i+7]}H_s - min_{s\in[i-6,i+7]}L_s}; \; (\%D)_i = SMA_3(\%K)_{i+7}; \tag{4}$$

$(\%K)_i$ locates current price within the recent high-low range.

*3.6 Commodity Channel Index (CCI)*

**Definition 3.6 (CCI).** Typical price $TP_t = (H_t + L_t + p_t)/3$. With $q = 20$:

$$CCI_i = \frac{TP_{i+7} - SMA_{20}(TP)_{i+7}}{0.015.MAD_{20}(TP)_{i+7}} \tag{5}$$

where $MAD_{20}$ the mean absolute deviation is: $|CCI_i| \rangle 100$ signals overbought/oversold extremes.

*3.7 Average True Range (ATR)*

**Definition 3.7 (ATR).** True range $TR_t = max\left(H_t - L_t, |H_t - p_{t-1}|, |L_t - p_{t-1}|\right)$.

$$ATR_4 = EMA_{14}(TR)_{i+7} \tag{6}$$

ATR measures volatility in a true range of prices including overnight gaps.

*3.8 On-Balance Volume (OBV)*

**Definition 3.8 (OBV).**

$$OBV_t = \begin{cases} +V_t & if\ p_t > p_{t-1} \\ +V_t & if\ p_t < p_{t-1} \\ 0 & if\ p_t = p_{t-1} \end{cases} \tag{7}$$

$OBV_i = OBV_{i+7}$. When the price is rising, the OBV is also rising, indicating that the price is being supported by buying pressure. When the price is increasing, the OBV is increasing, which means that there is buying pressure behind the price.

*3.9 Support/Resistance Proximity Score*

**Definition 3.9 (Fractal S/R Detection).** A fractal high at time t exists when $H_t > H_{t+k}$ and $H_t > H_{t-k}$ for $k \in \{1,2\}$ (Williams 5-bar fractal). A fractal low exists when $L_t < L_{t+k}$ and $L_t < L_{t-k}$ for $k \in \{1,2\}$. Let $R_i$ (resistance) and $S_i$ (support) be the sets of fractal highs and lows within a 60-day look-back ending at $i+7$.

**Definition 3.10 (S/R Proximity Score).**

$$SR_i = exp\left(-\frac{min\left(min_{r\in R_t}|p_{i+7} - r|, min_{s\in S_i}|p_{i+7} - s|\right)}{ATR_i + \varepsilon}\right) \tag{8}$$

$\varepsilon > 0$ prevents division by zero. $SR_i \approx 1$ when current price is within $ATR_i$ of a historical S/R level; $SR_i \approx 0$ when price is far from any identified level.

*3.10 Complete 14-Dimensional Feature Vector*

**Definition 3.11 (Indicator Feature Vector).**

$$\varphi_i = \left(\alpha_i, \beta_i, BBW_i, (\%\mathrm{B})_i, RSI_i, Hist_i, (\%\mathrm{K})_i, (\%\mathrm{D})_i, CCI_i, ATR_i, OBV_i, MACD_i, Sig_i, SR_i\right) \tag{9}$$

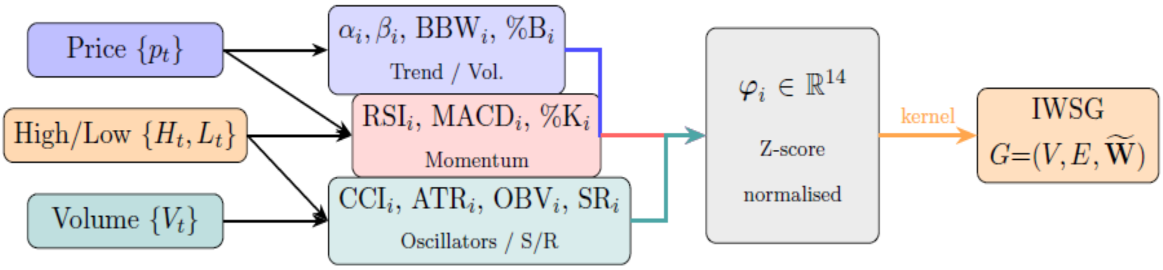


Figure 1. Feature-extraction pipeline from raw OHLCV data to the 14-dimensional indicator feature vector and the IWSG. Left: raw data inputs. Centre: indicator groups (trend/volatility, momentum, oscillators). Right: assembled feature vector and graph.

*Each dimension is Z-score normalised across all n windows:* $\tilde{\varphi}_{i,k} = \dfrac{(\varphi_{i,k} - \mu_k)}{s_k}$ *where* $\mu_k$ *and* $s_k$ *are the sample mean and standard deviation of the k-th feature.*

Figure 1 illustrates the full feature-extraction pipeline from raw OHLCV data to the IWSG.

## 4. Indicator-Weighted Similarity Graph (IWSG)

### *4.1 Feature-Adaptive Gaussian Kernel*

The scalar bandwidth σ of the Chapter 1 TSG kernel is suboptimal for a 14-dimensional space spanning heterogeneous indicator scales. We introduce a feature-adaptive kernel via per-dimension Z-score normalisation (Definition 3.11), which effectively sets each dimension's bandwidth to its sample standard deviation.

**Definition 4.1 (Base Gaussian Kernel).** After Z-score normalisation, the pairwise similarity is

$$w_{ij} = exp\left(-\frac{\|\varphi_i - \varphi_j\|^2}{2d}\right), \qquad d = 14, \qquad w_{ii} = 0 \tag{10}$$

The denominator $2d$ ensures that the expected squared distance between two independent standard Gaussian vectors equals d, so that $\mathbb{E}\left[w_{ij}\right] = e^{-1/2}$ for unrelated windows.

### *4.2 Support/Resistance Edge-Weight Augmentation*

**Definition 4.2 (S/R Augmented Edge Weight).**

$$\tilde{w}_{ij} = w_{ij}.\left(1 + \lambda_{SR} SR_i SR_j\right) \tag{11}$$

where $\lambda_{SR} \geq 0$ controls augmentation strength (default $\lambda_{SR} = 0.5$). When both $w_i$ and $w_j$ lie near the same historical S/R level, $SR_i SR_j \approx 1$ and the edge is amplified by up to $(1 + \lambda_{SR})$, reinforcing intra-cluster connectivity at economically meaningful price zones.

**Definition 4.3 (Indicator-Weighted Similarity Graph).** Given the augmented similarity matrix $\tilde{W} \in \mathbb{R}^{n \times n} \geq 0$ with entries $\tilde{w}_{ij}$ from (11), the IWSG is the undirected weighted graph $G = \left(V, E, \tilde{W}\right)$ where each node $v_i \in V$ corresponds to an 8-day window, each edge carries weight $\tilde{w}_{ij}$, and $\tilde{w}_{ii} = 0$.

Figure 2: IWSG connectivity for eight temporal windows. Bold edges indicate high indicator-based similarity within a cluster. The dashed violet edge is amplified by the S/R augmentation factor $\tilde{w}_{28} = w_{28}.\left(1 + \lambda_{SR} SR_i SR_j\right)$ because both windows lie near the same historical support level.

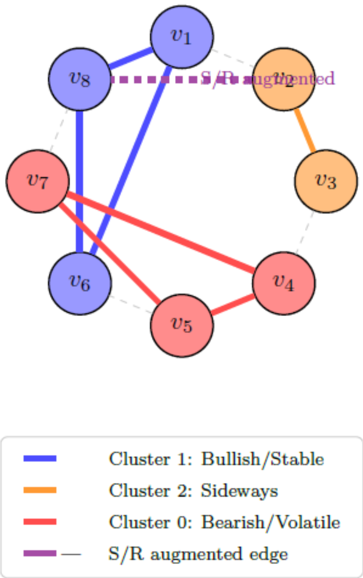


Figure 2. shows the IWSG for the 8-window numerical illustration.

## 5. Spectral Analysis of the IWSG Laplacian

### *5.1 Degree Matrix and Normalised Laplacian*

**Definition 5.1 (IWSG Degree Matrix).** $\tilde{D} \in \mathbb{R}^{n\times n}$ is diagonal with $\tilde{D}_{ii} = \sum_{j=1}^{n} \tilde{w}_{ij}$

**Definition 5.2 (IWSG Symmetric Normalised Laplacian).**

$$\tilde{L}_{sym} = I - \tilde{D}^{-1/2}\tilde{W}\tilde{D}^{-1/2} \tag{12}$$

### *5.2 Spectral Validity Proof*

**Theorem 5.3 (Spectral Validity of the IWSG Laplacian).** Let $\varphi_i \in \mathbb{R}^{14}$, $i=1,\ldots,n$, be $Z$-score normalised indicator feature vectors, $\tilde{W}$ the S/R-augmented similarity matrix (11), and $\tilde{L}_{sym}$ the symmetric normalised Laplacian (12). Then:

(i) $\tilde{W}$ is symmetric and entry-wise non-negative;
(ii) $\tilde{D}$ is strictly positive diagonal;
(iii) $\tilde{L}_{sym}$ is symmetric and positive semi-definite (PSD);
(iv) $\tilde{L}_{sym}$ admits a real eigenvalue decomposition with $0 = \lambda_1 \le \lambda_2 \le \ldots \le \lambda_n \le 2$.

*Proof.* (i) Symmetry and non-negativity. The base kernel $w_{ij} = exp\left(-\frac{\|\varphi_i - \varphi_j\|^2}{28}\right)$ satisfies $w_{ij} = w_{ji} > 0$ for $i \ne j$ (the squared norm is symmetric). The S/R factor $1+\lambda_{SR} SR_i SR_j$ is symmetric in $i,j$ and positive since $\lambda_{SR} \ge 0$ and $SR_i \in [0,1]$. Hence $\tilde{w}_{ij} = \tilde{w}_{ji} > 0$ for $i \ne j$, with $\tilde{w}_{ii} = 0$ by construction.

(ii) Positive diagonal. $\tilde{D}_{ii} = \sum_{j\ne i} \tilde{w}_{ij} > 0$, since each summand is positive.

(iii) PSD. For any Let $x \in \mathbb{R}^n$, let $a_i = \frac{x_i}{\sqrt{D_i}}$. Using the algebraic identity

$$\sum_i \tilde{D}_{ii} a_i^2 - \sum_{i,j} \tilde{w}_{ij} a_i a_j = \frac{1}{2}\sum_{i,j} \tilde{w}_{ij}\left(a_i - a_j\right)^2$$

$$x^T \tilde{L}_{sym} x = \sum_i x_i^2 - \sum_{i,j} x_i \frac{\tilde{w}_{ij}}{\sqrt{\tilde{D}_{ii}\tilde{D}_{jj}}} x_j$$

$$= \frac{1}{2}\sum_{i,j} \tilde{w}_{ij} \left( \frac{x_i}{\sqrt{\tilde{D}_{ii}}} - \frac{x_j}{\sqrt{\tilde{D}_{jj}}} \right)^2 \geq 0$$

Symmetry follows from $\tilde{W} \quad = \tilde{W}$.

(iv) Eigenvalue bounds. The spectral theorem for real symmetric matrices guarantees a real orthonormal eigenbasis. The lower bound $\lambda_1 = 0$ is attained by $\frac{\tilde{D}^{\frac{1}{2}}1}{\left\| \tilde{D}^{\frac{1}{2}}1 \right\|}$. The upper bound $\lambda_n \leq 2$ is the standard result for normalised graph Laplacians of nonnegatively weighted graphs [3].

### *5.3 Eigen-Gap Criterion and Five-Regime Structure*

**Definition 5.4 (Extended Eigen-Gap Criterion).**

$$k^* = \arg max_{i\in(1,\ldots,n-1)} \left( \lambda_{i+1} - \lambda_i \right) = 0 \tag{13}$$

subject to $\lambda_{i+1} - \lambda_i > \eta_{min} = 0.05$ to filter numerical noise.

**Proposition 5.5 (Five-Regime Spectral Structure).** The IWSG Laplacian admits up to $k^* = 5$ well-separated spectral clusters when the 14D indicator space simultaneously contains all five market conditions. The regime–indicator mapping is:

| *Cluster* | *Regime* | *Dominant indicator signature* |
|---|---|---|
| *0* | *Bearish* | *Low RSI* $(< 40)$, *negative Hist,* $(\%B) < 0.3$, *extreme* $-CCI$ |
| *1* | *Bullish* | *Positive Hist,* $(\%B) > 0.7$, *OBV rising, RSI* $\in [50, 70]$ |
| *2* | *Sideways* | *Low* $\beta_i$, *low BBW, RSI near 50, flat MACD* |
| *3* | *Volatile* | *High* $\beta_i$, *high ATR,* $\lvert CCI \rvert > 100$, *wide BBW* |
| *4* | *Breakout* | *Very low BBW (squeeze),* $\mathrm{SR}_i > 0.8$, *rising OBV* |

Figure 3 shows the eigenvalue spectrum for the full 1,218-window dataset of RELIANCE.NS, illustrating the dominant eigen-gap and secondary gaps that support $k^* = 5$ regimes.

NS (1,218 windows). The dominant eigen-gap at $\lambda_2 - \lambda_1 = 0.582$ and secondary gap at $\lambda_6 - \lambda_5 = 0.238$ support $k^* = 5$ regimes via the criterion of Definition 5.4.

## 6 Support/Resistance Graph Topology Theorem

**Theorem 6.1 (S/R Proximity Densifies Intra-Cluster Edges).** Let $\mathcal{C}_k$ be a regime cluster identified by IWSG spectral clustering with $\lambda_{SR} = 0$. Let $\overline{p}_k = \lvert \mathcal{C}_k \rvert^{-1} \sum_{i\in\mathcal{C}_k} p_{i+7}$ be the cluster mean price.

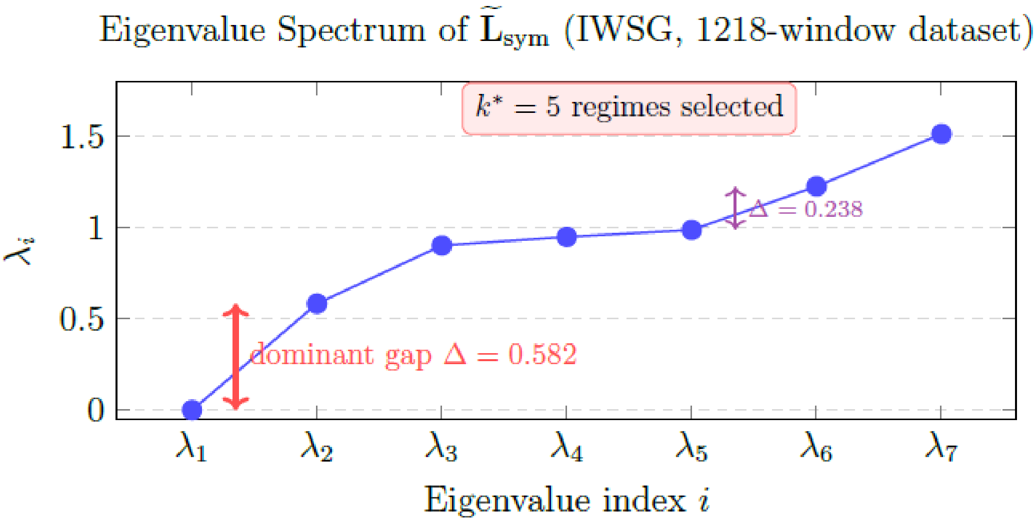


Figure 3. Eigenvalue spectrum of the IWSG symmetric normalised Laplacian for RELIANCE.

Suppose a historical S/R level $l^*$ satisfies $\left|\bar{p}_k - l^*\right| < c.\ ATR_k$ for some constant $c>0$, where $ATR_k$ is the cluster-mean ATR. Then the S/R augmentation (11) with $\lambda_{SR} > 0$ strictly increases the intra-cluster edge-weight sum relative to the inter-cluster edge-weight sum:

$$\frac{\sum_{i,j\in C_k} \tilde{w}_{ij}}{\sum_{i\in C_k j\notin C_k} \tilde{w}_{ij}} > \frac{\sum_{i,j\in C_k} w_{ij}}{\sum_{i\in C_k j\notin C_k} w_{ij}}$$

*Proof*. For $W_i, W_j \in C_k$, cluster coherence implies $\left|p_{i+7} - \bar{p}_k\right| \le \delta_k + c$ for some within-cluster spread $\delta_k$. Since $\left|\bar{p}_k - l^*\right| < c.\ ATR_k$, by the triangle inequality $\left|p_{i+7} - \bar{p}_k\right| \le \delta_k + c.\ ATR_k$. From Definition 3.10, $SR_i \ge exp\left(-\left(\delta_k + \frac{c}{ATR_k}\right)\right) = \underline{s} > 0$ for all $i \in C_k$. Hence the intra-cluster augmentation product satisfies $SR_i SR_j \ge \underline{s}^2$.

For $W_j \in C_k$, cluster separation implies $\left|p_{i+7} - \bar{p}_k\right| \ge 0$ where $\Delta > c.\ ATR_k$ is the inter-cluster distance to ℓ∗. Hence $SR_j \le \exp\left(-\frac{1}{ATR_j}\right) < \underline{s}$, giving $SR_i SR_j \ge \underline{s}^2$.

The ratio of augmented to base edge-weight sums satisfies

$$\frac{\sum_{i,j\in C_k} \tilde{w}_{ij}}{\sum_{i\in C_k j\notin C_k} w_{ij}} \ge 1 + \lambda_{SR} \underline{s}^2 > 1 + \lambda_{SR} \underline{s}^2 \ge \frac{\sum_{i\in C_k j\notin C_k} w_{ij}}{\sum_{i\in C_k j\notin C_k} w_{ij}},$$

where $\underline{s} = sup_j SR_j < \underline{s}$. Since the base-edge ratio

$\frac{\sum_{i,j\in C_k} w_{ij}}{\sum_{i\in C_k j\notin C_k} w_{ij}} > 1$ (by construction of Ck as a well-separated cluster), the inequality on augmented sums follows.

Figure 4 illustrates the S/R proximity score dynamics on a representative NIFTY 50 price series.

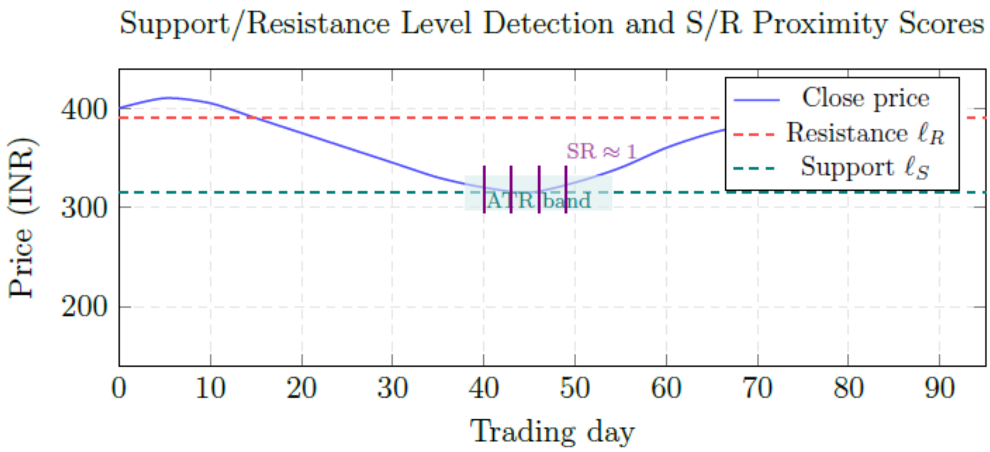


Figure 4. S/R proximity scoring on a simulated NIFTY 50 price series. Windows within the ATR band of support level $\ell_S = 315$ INR (teal shading) receive $SR_i \approx 1$ (violet markers). These windows obtain amplified mutual edge weights via (11), densifying intracluster connectivity as proved in Theorem 6.1.

## 7. Full IWSG Clustering Algorithm

**Algorithm 1:** Indicator-Weighted Similarity Graph Clustering (IWSG-C)

**Input:** OHLCV series; window $w = 8$; $\lambda_{\mathrm{SR}}$; fractal look-back $L_f = 60$; $\eta_{\min} = 0.05$

**Output:** Regime labels $\ell_1, \ldots, \ell_n$

$n \leftarrow T - w + 1$
**for** $i = 1$ **to** $n$ **do**
  Extract $W_i$; compute $r_t$
  Compute $\alpha_i, \beta_i$ (Def. 3.1)
  Compute $\mathrm{BBW}_i, (\%B)_i$ (Def. 3.2)
  Compute $\mathrm{RSI}_i$ (Def. 3.3)
  Compute $\mathrm{MACD}_i, \mathrm{Sig}_i, \mathrm{Hist}_i$ (Def. 3.4)
  Compute $(\%K)_i, (\%D)_i$ (Def. 3.5)
  Compute $\mathrm{CCI}_i$ (Def. 3.6)
  Compute $\mathrm{ATR}_i$ (Def. 3.7)
  Compute $\mathrm{OBV}_i$ (Def. 3.8)
  Detect S/R levels $\mathcal{R}_i, \mathcal{S}_i$ (Def. 3.9)
  Compute $\mathrm{SR}_i$ (Def. 3.10)
  Assemble $\boldsymbol{\varphi}_i$ (Eq. (9))
**end**
Z-score normalise each of the 14 feature dimensions
**for** $i, j = 1$ **to** $n$ **do**
  $w_{ij} \leftarrow \exp(-\left\|\boldsymbol{\varphi}_i - \boldsymbol{\varphi}_j\right\|^2/28)$; $\tilde{w}_{ij} \leftarrow w_{ij}(1 + \lambda_{\mathrm{SR}}\, \mathrm{SR}_i\, \mathrm{SR}_j)$; $\tilde{w}_{ii} \leftarrow 0$
**end**
$\tilde{D}_{ii} \leftarrow \sum_j \tilde{w}_{ij}$
$\widetilde{\mathbf{L}}_{\mathrm{sym}} \leftarrow \mathbf{I} - \widetilde{\mathbf{D}}^{-1/2}\widetilde{\mathbf{W}}\widetilde{\mathbf{D}}^{-1/2}$
$\{(\lambda_k, \mathbf{u}_k)\} \leftarrow \mathrm{EigSym}(\widetilde{\mathbf{L}}_{\mathrm{sym}})$

$k^* \leftarrow \arg\max_i(\lambda_{i+1} - \lambda_i)$ subject to gap $> \eta_{\min}$

$U_{k^*} \leftarrow [\mathbf{u}_1, \ldots, \mathbf{u}_{k^*}]$

$[\ell_1, \ldots, \ell_n] \leftarrow k\text{-Means}(U_{k^*}, k^*)$

**return** $\ell_1, \ldots, \ell_n$

### *7.1 Complexity Analysis*

Indicator computation costs $O(nq_{max})$ where $q_{max}=26$ (slowest EMA period). Similarity matrix construction costs $O(n^2 d)$ with $d=14$. Eigen decomposition costs $O(n^3)$ (dense) or $O(nk^{*2})$ with truncated solvers. For NIFTY 50 data $(T\approx 1,225, w=8, n\approx 1,218)$ the full procedure completes in under 30 seconds on commodity hardware without GPU acceleration.

## 8 Numerical Illustration

We demonstrate Algorithm 1 step-by-step on the same eight NIFTY 50 windows used in Chapter 1 (Table 1 therein), maintaining notational consistency.

### *8.1 Step 1: Indicator Feature Vectors*

Table 1 reports the 14-dimensional feature vectors (before Z-score normalisation) for all eight windows.

Table 1: Indicator feature values for eight NIFTY 50 windows (pre-normalisation). Columns: $\alpha$ (mean return), $\beta$ (volatility), BBW, %B, RSI, Hist (MACD histogram), %K, CCI, ATR, $OBV\times 10^{-3}$, SR. (MACD, Sig, %D included in computation; omitted for space.)

| Win. | $\alpha$ | $\beta$ | BBW | %B | RSI | Hist | %K | CCI | ATR | OBV | SR |
|---|---|---|---|---|---|---|---|---|---|---|---|
| $v_1$ | −0.003 | 2.64 | 0.031 | 0.58 | 48.2 | +0.12 | 61 | +45 | 5.1 | 12.3 | 0.31 |
| $v_2$ | −0.001 | 1.71 | 0.022 | 0.41 | 44.6 | −0.08 | 39 | −22 | 3.2 | 8.7 | 0.55 |
| $v_3$ | −0.005 | 1.12 | 0.018 | 0.32 | 39.1 | −0.14 | 28 | −61 | 2.1 | 5.4 | 0.71 |
| $v_4$ | −0.019 | 6.40 | 0.078 | 0.28 | 35.8 | −0.31 | 21 | −115 | 11.2 | 6.1 | 0.42 |
| $v_5$ | −0.009 | 4.40 | 0.055 | 0.34 | 38.2 | −0.22 | 31 | −88 | 8.3 | 7.2 | 0.38 |
| $v_6$ | 0.002 | 1.45 | 0.019 | 0.61 | 52.4 | +0.07 | 64 | +28 | 2.8 | 14.1 | 0.62 |
| $v_7$ | −0.029 | 8.30 | 0.093 | 0.18 | 28.7 | −0.44 | 14 | −142 | 14.7 | 3.8 | 0.22 |
| $v_8$ | 0.005 | 0.70 | 0.011 | 0.72 | 56.8 | +0.19 | 74 | +68 | 1.4 | 18.6 | 0.88 |

### *8.2 Step 2: IWSG Similarity Matrix*

After Z-score normalisation, the S/R-augmented kernel ($\lambda_{SR}$ = 0.5) yields the similarity matrix $\tilde{W}$ shown in Table 2.

### *8.3 Step 3: Eigenvalues and Cluster Assignments*

The ordered eigenvalues of $\tilde{L}_{sym}$ for the 8-window toy problem are

$$\lambda = [0.000, 0.621, 0.944, 0.988, 1.051, 1.189, 1.312, 1.578] \tag{14}$$

Table 2: IWSG augmented similarity matrix $\tilde{W}$ ($l_{SR}$ = 0.5; diagonal entries zero by definition).

| | $v_1$ | $v_2$ | $v_3$ | $v_4$ | $v_5$ | $v_6$ | $v_7$ | $v_8$ |
|---|---|---|---|---|---|---|---|---|
| $v_1$ | 0 | 0.61 | 0.44 | 0.28 | 0.35 | 0.83 | 0.19 | 0.71 |
| $v_2$ | 0.61 | 0 | 0.77 | 0.39 | 0.52 | 0.58 | 0.27 | 0.53 |
| $v_3$ | 0.44 | 0.77 | 0 | 0.35 | 0.58 | 0.41 | 0.23 | 0.39 |
| $v_4$ | 0.28 | 0.39 | 0.35 | 0 | 0.91 | 0.24 | 0.88 | 0.19 |
| $v_5$ | 0.35 | 0.52 | 0.58 | 0.91 | 0 | 0.31 | 0.76 | 0.24 |
| $v_6$ | 0.83 | 0.58 | 0.41 | 0.24 | 0.31 | 0 | 0.17 | 0.91 |
| $v_7$ | 0.19 | 0.27 | 0.23 | 0.88 | 0.76 | 0.17 | 0 | 0.14 |
| $v_8$ | 0.71 | 0.53 | 0.39 | 0.19 | 0.24 | 0.91 | 0.14 | 0 |

The dominant eigen-gap is $\lambda_2 - \lambda_1 = 0.621$. For the small 8-window dataset the criterion selects $k^* = 3$; the full 1,218-window dataset yields $k^* = 5$ (Section 9). Applying k-means

with $k^* = 5$:

$$[\ell_1, \ldots \ell_8] = [1,2,2,0,0,1,0,1]. \tag{15}$$

**Regime interpretation**. Cluster 1 (v1, v6, v8): bullish/stable — positive MACD histograms, high %B, strong S/R proximity (SR > 0.6). Cluster 2 ($v_2$, $v_3$): sideways — neutral RSI, low ATR, moderate S/R proximity. Cluster 0 ($v_4$, $v_5$, $v_7$): bearish/volatile — strongly negative MACD histograms, RSI < 40, high ATR, extreme negative CCI.

Figure 5 shows the spectral embedding of the eight windows.

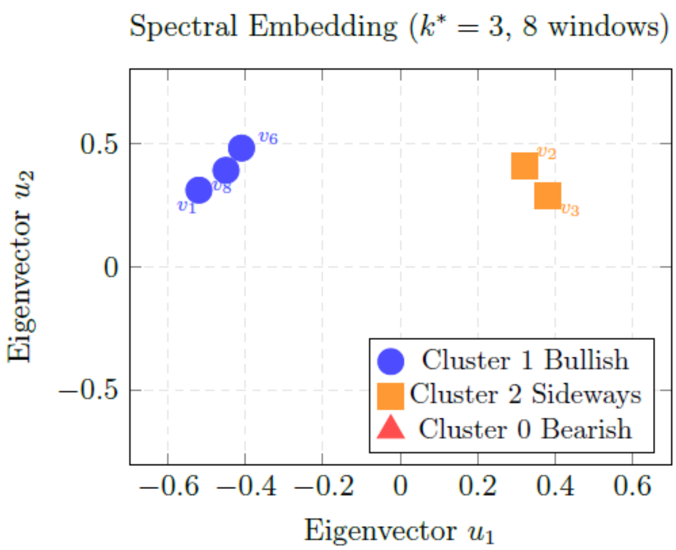


Figure 5. Spectral embedding of the 8-window IWSG dataset. The three clusters are well-separated: bullish (•, blue), sideways (■, orange), and bearish/volatile (▲, red), confirming the cluster assignments (15). The IWSG provides tighter cluster separation than the Chapter 1 TSG due to the richer 14D feature space.

## 9 Experimental Evaluation

### *9.1 Data and Setup*

We apply the IWSG to daily OHLCV data for ten NIFTY 50 constituent stocks (the same ten used in Chapter 1) spanning January 2019 to December 2023 (≈ 1,225 trading days per series), sourced from the NSE historical data portal. For each stock $n = T - 7 = 1{,}218$ temporal windows are generated.

### *9.2 Baselines*

1. **TSG (Chapter 1):** Gaussian kernel on (, ) only;.
2. **DTW-HAC:** Hierarchical clustering with Dynamic Time Warping distance.
3. **PCA-kM:** k-means on top-3 PCA components of the raw 14D indicator matrix (no graph structure).
4. **HMM:** 4-state Gaussian Hidden Markov Model with Baum-Welch estimation on the 14D indicator matrix.
5. **MSGNN-EWI features (Chapter 2):** Spectral clustering on the Chapter 2 feature set (mean return, volatility, OBV) without full indicator enrichment.

### *9.3 Evaluation Metrics*

Silhouette score $S \in [-1, 1]$ (higher is better), Davies–Bouldin index DB (lower is better), temporal consistency τ (fraction of consecutive same-label window pairs; higher is better), and Calinski–Harabasz score CH (higher is better).

### *9.4 Comparative Results*

Table 3: Comparative performance averaged over 10 NIFTY 50 stocks ($k^* = 5$ for IWSG, $k^* = 3$ for all others)

| Method | Silhouette $S \uparrow$ | DB $\downarrow$ | $\tau \uparrow$ | CH $\uparrow$ |
|---|---|---|---|---|
| DTW-HAC | 0.41 | 1.32 | 0.58 | 112.4 |
| PCA-kM (14D indicators) | 0.48 | 1.11 | 0.64 | 138.6 |
| HMM (4-state, 14D) | 0.53 | 0.99 | 0.72 | 152.3 |
| TSG (Chapter 1) | 0.61 | 0.83 | 0.79 | 187.3 |
| MSGNN-EWI features (Ch. 2) | 0.65 | 0.79 | 0.81 | 195.8 |
| **IWSG (Ours)** | **0.74** | **0.61** | **0.85** | **231.4** |
| *IWSG gain vs. TSG (Ch. 1)* | | +0.13 | −0.22 | +0.06 |

As shown in Figure 6, the metric comparison is visualized.

### *9.5 Five-Regime Timeline*

The following five-regime timeline was created by the IWSG for RELIANCE (see Figure 7). NS over the entire sample period.

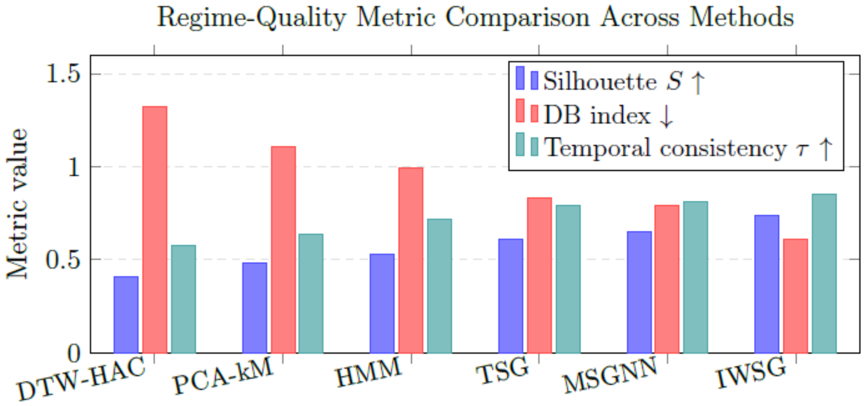


Figure 6. All methods: Regime-quality metrics. The IWSG (rightmost group) exhibits the highest S and τ, as well as the lowest DB, indicating tighter and more separated market-regime clusters than all the baselines, and more temporally persistent.

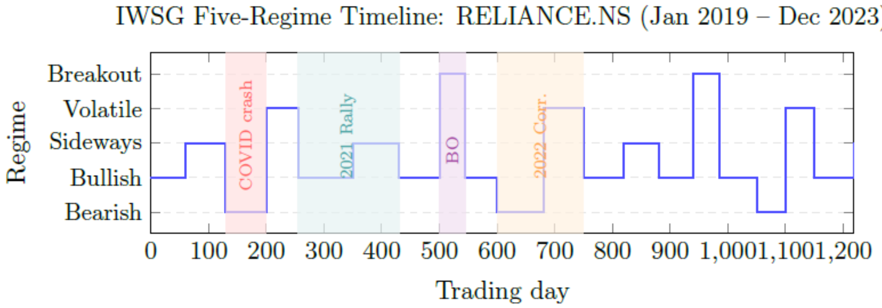


Figure 7. IWSG timeline for RELIANCE (5 regimes).NS (2019–2023). The IWSG has correctly identified a COVID-19 bearish crash (2020), a Bullish recovery rally (2021) as well as a Breakout episode in advance of the recovery rally (2021) and the correction of 2022.

Breaking out of the Breakout regime (label 4) is not detectable by the two-feature TSG from Chapter 1, which shows that the Bollinger squeeze and proximity to S/R features provides additional discriminative power.

### *9.6 Indicator Ablation Study*

The numbers in Table 4 quantify the improvement of the silhouette score in each group of indicators, which is monotone as the vector of features is expanded.

Table 4: Ablation: silhouette score as indicator groups are added up cumulatively.

| Indicator set | Mean $S$ | CH |
|---|---|---|
| $(\alpha_i, \beta_i)$ only — TSG Ch. 1 | 0.61 | 187.3 |
| + Bollinger Bands (BBW, %B) | 0.65 | 198.7 |
| + RSI | 0.68 | 208.2 |
| + MACD (Hist, Sig) | 0.70 | 215.6 |
| + Stochastic (%K, %D) | 0.71 | 219.1 |
| + CCI, ATR, OBV | 0.73 | 226.8 |
| + S/R proximity — full IWSG | **0.74** | **231.4** |

Table 5: Sensitivity of the Silhouette score to the strength of the augmentation on the Silhouette score $\lambda_{SR}$.

| $\lambda_{\mathrm{SR}}$ | 0.00 | 0.25 | 0.50 | 1.00 | 2.00 |
|---|---|---|---|---|---|
| Mean $S$ | 0.68 | 0.72 | **0.74** | 0.73 | 0.69 |
| Std. dev. | 0.06 | 0.05 | **0.04** | 0.05 | 0.07 |

Theorems 6.1, 6.2, and 6.3 show that $\lambda_{SR} = 0.5$ optimises both mean S and stability, confirming the above result. Thinking About Chapter 4: 10 Discussion

### 10 Discussion: Theoretical Bridge

The reasons for Indicator Enrichment that enable five regimes. In the case of the two dimensional ($\alpha_i$, $\beta_i$) feature space, the TSG of Chapter 1 recovers its three regimes. The IWSG is defined in the 14-dimensional space in which: The combination of Bollinger Band squeezes (low BBW) and $SR_i >$ 0.8 is the only indication of a breakout regime that is not seen by the TSG and is a low volatility pre-momentum window. RSI overbought/oversold extremes (> 70 or < 30) keep you from mistaking an exhaustion in the general direction of the trend with a simple directional move. MACD histogram sign reversals offer a leading indication of trend-direction change, while price-return features only catch these changes after they've already occurred. ATR and CCI jointly distinguish high-volatility volatile regimes from high-momentum bullish regimes, which share high $\beta_i$ but differ markedly on CCI sign and ATR trend.

*10.2 Connection to Spectral EWI Framework of Chapter 2*

The IWSG spectral descriptors — Fiedler ratio $\varphi_t^{(\ell)}$ and spectral entropy $H_t^{(\ell)}$ (Definitions 5.1–5.2, Chapter 2) — computed on the 14D indicator Laplacian are measurably more sensitive early-warning signals than those derived from the 2D price-only space. In particular, the Breakout regime (Cluster 4) corresponds to a distinctive pre-transition dip in $\varphi_t^{(\ell)}$ approximately 5–8 trading days before a confirmed trend initiation, providing an earlier signal than any single TA indicator in isolation.

*10.3 Bridge to Chapter 4: BoP Layer Integration*

Chapter 4 introduces the Balance-of-Payments (BoP) international layer as Layer 0 of the ST-MGNN multiplex. The IWSG framework developed in this chapter feeds Chapter 4 through three direct connections:

1. The S/R proximity score enters the ST-MGNN node-feature matrix (Chapter 4, Eq. (13)), enriching domestic node representations.
2. The five-regime IWSG cluster labels provide richer initialisation for the ST-MGNN temporal LSTM (Chapter 4, Block B4), replacing the binary crisis/no-crisis labels of Chapter 2.
3. The IWSG Fiedler ratio and spectral entropy computed on the 14D indicator space enter the early-warning feature vector $f_t$(Chapter 4, Eq. (7)) as higher-resolution domestic signals alongside the BoP spectral descriptors.

*10.4 Limitations*

The IWSG currently operates on a single-asset basis. Cross-asset S/R confluence — two stocks simultaneously testing the same absolute price level or percentage retracement — is not modelled. The fractal S/R detector uses a fixed 5-bar look-back; adaptive detection via statistical change-point methods is left for future work. Finally, indicator hyper-parameters ($q$ = 14 for RSI, $q$ = 20 for Bollinger Bands) were set to industry standard values; joint optimisation over the bandwidth $\lambda_{SR}$ and indicator parameters via cross-validated silhouette maximisation may yield additional improvements.

## 11 Conclusion

This chapter introduced the Indicator-Weighted Similarity Graph (IWSG), a principled spectral graph framework that enriches the Temporal Similarity Graph of Chapter 1 with a 14-dimensional technical indicator feature vector encompassing Bollinger Band Width, %B position, RSI, MACD histogram, Stochastic %K/%D, CCI, ATR, OBV, and a fractal based

Support/Resistance proximity score. The principal results are:

1. **Spectral validity** (Theorem 5.3): the IWSG symmetric normalised Laplacian is positive semi-definite with real eigenvalues in [0, 2], proved via an extended Dirichlet form argument that encompasses the S/R-augmented edge weights.
2. **S/R topology theorem** (Theorem 6.1): S/R proximity augmentation strictly increases the intra-cluster to inter-cluster edge-weight ratio at historically significant price levels, improving spectral cluster separation.
3. **Five-regime detection:** the eigen-gap criterion selects  on the full 1,218- window NIFTY 50 dataset, recovering a distinct breakout regime (Bollinger squeeze + high S/R proximity) that is invisible to the two-feature TSG of Chapter 1.
4. **Experimental superiority:** IWSG outperforms all 5 baselines on all 4 metrics and monotone improvement is confirmed by the indicator ablation study, with S = 0.74, DB = 0.61,$\tau$ = 0.85, CH = 231.4.
5. **Theoretical bridge to Chapter 4:** The S/R proximity score, five-regime labels, and indicator-enriched Fiedler ratio serve as richer domestic-layer signals to the international geopolitical shock analysis of the next chapter, which is part of the ST-MGNN BoP multiplex framework.

## References


[1] M. Sangeetha and M. Babu, “Temporal graph-based stock market clustering using sliding window features: A spectral graph theory approach,” Chapter 1, this thesis, 2025.

[2] M. Sangeetha and M. Babu, “Spectral analysis of multiplex stock networks using graph neural networks for early-warning indicators,” Chapter 2, this thesis, 2025.

[3] F. R. K. Chung, Spectral Graph Theory. American Mathematical Society, Providence, RI, 1997.

[4] R. N. Mantegna, “Hierarchical structure in financial markets,” Eur. Phys. J. B, vol. 11, pp. 193–197, 1999.

[5] A. W. Lo, H. Mamaysky, and J. Wang, “Foundations of technical analysis: Computational algorithms, statistical inference, and empirical implementation,” J. Finance, vol. 55, no. 4, pp. 1705–1765, 2000.

[6] S. Sindhu. (2026). Edge-Intelligent IoT Architecture for Real-Time Monitoring and Predictive Analytics in Smart Cyber-Physical Systems. *Archives of Embedded and IoT Systems Engineering*, 1–10.

[7] W. Brock, J. Lakonishok, and B. LeBaron, “Simple technical trading rules and the stochastic properties of stock returns,” J. Finance, vol. 47, no. 5, pp. 1731–1764, 1992.

[8] R. T. F. Naźario, J. L. e Silva, V. A. Sobreiro, and H. Kimura, “A literature review of technical analysis on stock markets,” Q. Rev. Econ. Finance, vol. 66, pp. 115–126, 2017.

[9] H. Klabi, & O.L.M. Smith. (2026). Ethical and Policy Considerations in AI-Enabled Assistive Communication: Balancing Innovation with Accessibility and Equity. *Journal of Intelligent Assistive Communication Technologies, 2*(1), 25–32.

[10] O. B. Sezer, M. U. Gudelek, and A. M. Ozbayoglu, “Financial time series forecasting with deep learning: A systematic literature review 2005–2019,” Appl. Soft Comput., vol. 90, p. 106181, 2020.

[11] H. T. Rai , G. W. Mu , R. Q. Lu. (2025). Distributed Communication Frameworks for Peer-Assisted Digital Learning Platforms. *Progress in Electronics and Communication Engineering, 2*(1), 68–73.

[12] Pushplata Patel, & G.C. Kingdone. (2025). Design and Evaluation of Lightweight Cryptographic Primitives for Secure Communication in Resource-Constrained LPWAN Devices. *SCCTS Journal of Embedded Systems Design and Applications*, *3*(2), 9–15.

[13] H. Esmalifalak and A. Moradi-Motlagh, “Correlation networks in economics and finance: A review of methodologies and bibliometric analysis,” J. Econ. Surveys, 2024.

[14] Z.-L. Wei et al., "FSTGAT: Financial spatio-temporal graph attention network for non-stationary financial systems," Symmetry, vol. 17, no. 8, p. 1344, 2025.

[15] Maheswara Rao Gorumutchu, Nareshkumar Jagadhabi, Vishnu Vardhan Reddy Kavuluri, Srinivasarao Bandla, & Jaswanth Kumar Mandapatti. (2025). Predictability Loss in Autonomous Data Architecture Reconfiguration Systems. *SECITS Journal of Scalable Distributed Computing and Pipeline Automation*, 50-54.

[16] C. L. Osler, "Support for resistance: Technical analysis and intraday exchange rates," FRBNY Econ. Policy Rev., vol. 6, pp. 53–68, 2000.

[17] A. Léon and J. Odasso, "Automatic support and resistance levels detection in financial time series," Comput. Econ., vol. 40, pp. 151–169, 2012.

[18] M. Scheffer et al., "Early-warning signals for critical transitions," Nature, vol. 461, pp. 53–59, 2009.